

Search for three-nucleon short-range correlations in nuclei

1

2 Z. Ye,^{1,2,3} P. Solvignon,^{4,5} P. Aguilera,⁶ Z. Ahmed,⁷ H. Albataineh,⁸ K. Allada,⁴ B. Anderson,⁹ D. Anez,¹⁰ K.
3 Aniol,¹¹ J. Annand,¹² J. Arrington,³ T. Averett,¹³ H. Baghdasaryan,¹ X. Bai,¹⁴ A. Beck,¹⁵ S. Beck,¹⁵ V. Bellini,¹⁶
4 F. Benmokhtar,¹⁷ A. Camsonne,⁴ C. Chen,¹⁸ J.-P. Chen,⁴ K. Chirapatpimol,¹ E. Cisbani,¹⁹ M. M. Dalton,^{1,4} A.
5 Daniel,²⁰ D. Day,¹ W. Deconinck,²¹ M. Defurne,²² D. Flay,²³ N. Fomin,²⁴ M. Friend,²⁵ S. Frullani,¹⁹ E. Fuchey,²³
6 F. Garibaldi,¹⁹ D. Gaskell,⁴ S. Gilad,²¹ R. Gilman,²⁶ S. Glamazdin,²⁷ C. Gu,¹ P. Guèye,¹⁸ C. Hanretty,¹
7 J.-O. Hansen,⁴ M. Hashemi Shabestari,¹ O. Hen,²⁸ D. W. Higinbotham,⁴ M. Huang,² S. Iqbal,¹¹ G. Jin,¹ N.
8 Kalantarians,¹ H. Kang,²⁹ A. Kelleher,²¹ I. Korover,²⁸ J. LeRose,⁴ J. Leckey,³⁰ R. Lindgren,¹ E. Long,⁹ J.
9 Mammei,³¹ D. J. Margaziotis,¹¹ P. Markowitz,³² D. Meekins,⁴ Z. Meziani,²³ R. Michaels,⁴ M. Mihovilovic,³³ N.
10 Muangma,²¹ C. Munoz Camacho,³⁴ D. Nguyen,¹ B. Norum,¹ Nuruzzaman,³⁵ K. Pan,²¹ S. Phillips,⁵ E. Piasetzky,²⁸
11 I. Pomerantz,^{28,36} M. Posik,²³ V. Punjabi,³⁷ X. Qian,² Y. Qiang,⁴ X. Qiu,³⁸ P. E. Reimer,³ A. Rakhman,⁷ S.
12 Riordan,^{1,39} G. Ron,⁴⁰ O. Rondon-Aramayo,¹ A. Saha,^{4,*} L. Selvy,⁹ A. Shahinyan,⁴¹ R. Shneor,²⁸ S. Sirca,⁴² K.
13 Slifer,⁵ N. Sparveris,²³ R. Subedi,¹ V. Sulkosky,²¹ D. Wang,¹ J. W. Watson,⁹ L. B. Weinstein,⁸ B. Wojtsekhowski,⁴
14 S. A. Wood,⁴ I. Yaron,²⁸ X. Zhan,³ J. Zhang,⁴ Y. W. Zhang,²⁶ B. Zhao,¹³ X. Zheng,¹ P. Zhu,⁴³ and R. Zielinski⁵

(The Jefferson Lab Hall A Collaboration)

¹University of Virginia, Charlottesville, VA 22904

²Duke University, Durham, NC 27708

³Physics Division, Argonne National Laboratory, Argonne, IL 60439

⁴Thomas Jefferson National Accelerator Facility, Newport News, VA 23606

⁵University of New Hampshire, Durham, NH 03824

⁶Institut de Physique Nucléaire (UMR 8608), CNRS/IN2P3 - Université Paris-Sud, F-91406 Orsay Cedex, France

⁷Syracuse University, Syracuse, NY 13244

⁸Old Dominion University, Norfolk, VA 23529

⁹Kent State University, Kent, OH 44242

¹⁰Saint Mary's University, Halifax, Nova Scotia, Canada

¹¹California State University, Los Angeles, Los Angeles, CA 90032

¹²University of Glasgow, Glasgow G12 8QQ, Scotland, United Kingdom

¹³College of William and Mary, Williamsburg, VA 23187

¹⁴China Institute of Atomic Energy, Beijing, China

¹⁵Nuclear Research Center Negev, Beer-Sheva, Israel

¹⁶Universita di Catania, Catania, Italy

¹⁷Duquesne University, Pittsburgh, PA 15282

¹⁸Hampton University, Hampton, VA 23668

¹⁹INFN, Sezione Sanità and Istituto Superiore di Sanità, 00161 Rome, Italy

²⁰Ohio University, Athens, OH 45701

²¹Massachusetts Institute of Technology, Cambridge, MA 02139

²²CEA Saclay, F-91191 Gif-sur-Yvette, France

²³Temple University, Philadelphia, PA 19122

²⁴University of Tennessee, Knoxville, TN 37996

²⁵Carnegie Mellon University, Pittsburgh, PA 15213

²⁶Rutgers, The State University of New Jersey, Piscataway, NJ 08855

²⁷Kharkov Institute of Physics and Technology, Kharkov 61108, Ukraine

²⁸Tel Aviv University, Tel Aviv 69978, Israel

²⁹Seoul National University, Seoul, Korea

³⁰Indiana University, Bloomington, IN 47405

³¹Virginia Polytechnic Inst. and State Univ., Blacksburg, VA 24061

³²Florida International University, Miami, FL 33199

³³Jozef Stefan Institute, Ljubljana, Slovenia

³⁴Université Blaise Pascal/IN2P3, F-63177 Aubière, France

³⁵Mississippi State University, Mississippi State, MS 39762

³⁶The University of Texas at Austin, Austin, Texas 78712

³⁷Norfolk State University, Norfolk, VA 23504

³⁸Lanzhou University, Lanzhou, China

³⁹University of Massachusetts, Amherst, MA 01006

⁴⁰Racah Institute of Physics, Hebrew University of Jerusalem, Jerusalem, Israel

⁴¹Yerevan Physics Institute, Yerevan 375036, Armenia

⁴²University of Ljubljana, Ljubljana, Slovenia

⁴³University of Science and Technology, Hefei, China

(Dated: August 17, 2017)

59

We present new data probing short-range correlations (SRCs) in nuclei through the measurement of electron scattering off high-momentum nucleons in light nuclei. The inclusive cross section ratios of $^4\text{He}/^3\text{He}$ and $^{12}\text{C}/^3\text{He}$ are observed to be both x and Q^2 independent for $1.5 < x < 2$, confirming the previously observed dominance of two-nucleon short-range correlations. The cross section ratios for $x > 2$ do not agree with an earlier measurement which suggested that three-nucleon correlations dominated the interaction in this Q^2 range. While 3N-SRCs may have an important contribution, these data suggest that they cannot be isolated in the same simple fashion as 2N-SRCs.

PACS numbers: 13.60.Hb, 25.10.+s, 25.30.Fj

Understanding the complex structure of the nucleus remains one of the major uncompleted tasks in nuclear physics, and significant questions remain about the high-momentum components of the nuclear wavefunction. This important aspect of nuclear structure is not described by the shell model description. This high-momentum strength appears at low momenta in Mean field calculations [1] which subsequently over predict the cross section for proton knock-out reactions below the Fermi momentum [2–4].

In the dense and energetic environment of the nucleus, nucleons have a significant probability of interacting at distances ≤ 1 fm, even in light nuclei [5, 6]. Protons and neutrons interacting through the strong, short-distance part of the NN interaction give rise to pairs of nucleons with large momenta. These high-momentum pairs, referred to as short-range correlations (SRCs), are the primary source of high-momenta in nuclei [7–9], well above the typical scale of the Fermi momentum ($k_F \approx 300$ MeV/c) associated with the shell model picture of nuclear structure. For momenta below k_F , we observe shell-model behavior which is strongly A dependent, while two-body physics dominates above k_F resulting in a universal structure for all nuclei that is steered by the details of the NN interaction [10–12].

In the case of inclusive electron scattering it is possible through kinematics, as follows, to isolate events in which the electron interacts with high-momentum nucleons. The electron transfers energy, ν , and momentum, \vec{q} , to the struck nucleon by exchanging a virtual photon with four momentum transfer $q^2 = -Q^2 = \nu^2 - |\vec{q}|^2$. It is useful in this case to define the kinematic variable $x = Q^2/(2M_p\nu)$, where M_p is the mass of the proton. Elastic scattering from a stationary proton corresponds to $x = 1$, while inelastic scattering must occur at $x < 1$. In a nucleus, the momentum of the nucleon produces a broad quasielastic peak centered near $x = 1$. Scattering at $x > 1$ is beyond the kinematic threshold for scattering from a free nucleon. At values of x slightly greater than unity, scattering can occur either from nucleons with the modest momenta expected from the mean field, or from high-momentum nucleons associated with SRCs. As x increases, larger initial momenta are required until scattering from nucleons below the Fermi momentum is kinematically forbidden, isolating scattering from high-momentum nucleons associated with SRCs [9–11, 13].

Because the momentum distribution of the nucleus is not a physical observable, one cannot directly extract and study its high-momentum component. One can, however, test the idea of a universal structure of the high-momentum components by comparing scattering from different nuclei at kinematics which require that the struck nucleon have a large initial momentum [10]. Previous measurements at SLAC and Jefferson Lab revealed a universal form to the high-momentum distributions of the struck nucleons [8, 9, 13–17]. In these experiments, the cross section ratios for inclusive scattering from heavy nuclei to the deuteron were shown to scale, i.e. be independent of x and Q^2 , for $x \gtrsim 1.5$ and $Q^2 \gtrsim 1.5$ GeV², corresponding to scattering from nucleons with momenta above 300 MeV/c. Other measurements have demonstrated that these high-momentum components are dominated by high-momentum n-p pairs [18–23], meaning that the high-momentum components in all nuclei have a deuteron-like structure. While final-state interactions (FSI) decrease with increasing Q^2 in inclusive scattering, FSI between nucleons in the correlated pair may not disappear. It is typically assumed that the FSI are identical for the deuteron and the deuteron-like pair in heavier nuclei, and thus cancel in these ratios [9, 10].

This approach can be extended to look for universal behavior arising from 3N-SRCs by examining scattering at $x > 2$ (beyond the kinematic limit for scattering from a deuteron). Within the simple SRC model [7], the cross section is composed of scattering from one-body, two-body, etc... configurations, with the one-body (shell-model) contributions dominating at $x \approx 1$, while 2N-SRCs (3N-SRCs) dominate as $x \rightarrow 2(3)$. Taking ratios of heavier nuclei to ^3He allows a similar examination of the target ratios for $x > 2$, where the simple SRC model predicts a universal behavior associated with three-nucleon SRCs (3N-SRCs) - configurations where three nucleons have large relative momenta but little total momentum. 3N-SRCs could come from either three-nucleon forces or multiple hard two-nucleon interactions. The first such measurement [14] observed x -independent ratios for $x > 2.25$. This was interpreted as a result of 3N-SRCs dominance in this region. However the ratios were extracted at relatively small Q^2 , and the Q^2 dependence was not measured. In the experiment of Ref. [15], at higher Q^2 , the $^4\text{He}/^3\text{He}$ ratios were significantly larger. Consequently, the question of whether 3N-SRC contribu-

tions have been cleanly identified and observed to dominate at some large momentum scale is as yet unanswered.

The results reported here are from JLab experiment E08-014 [24], which focused on precise measurements of the x and Q^2 dependence of the $A/{}^3\text{He}$ cross section ratios at large x . A 3.356 GeV electron beam with currents ranging from 40 to 120 μA impinged on nuclear targets, and scattered electrons were detected in two nearly identical High-Resolution Spectrometers (HRSs) [25]. Data were taken on six targets: three 20-cm cryogenic targets (liquid ${}^2\text{H}$ and gaseous ${}^3\text{He}$ and ${}^4\text{He}$) and thin foils of ${}^{12}\text{C}$, ${}^{40}\text{Ca}$ and ${}^{48}\text{Ca}$. We focus here on the results from the light nuclei, $A \leq 12$, which were taken to examine the 3N-SRC region, while the Calcium data were taken to examine the isospin dependence in the 2N-SRC kinematics.

Each HRS consists of a pair of vertical drift chambers (VDCs) for particle tracking, two scintillator planes for triggering and timing measurements, and a gas Čerenkov counter and two layers of lead-glass calorimeters for particle identification [25]. Scattering was measured at $\theta = 21^\circ, 23^\circ, 25^\circ$, and 28° , covering a Q^2 range of 1.3–2.2 GeV^2 . A detailed description of the experiment and data analysis can be found in Ref. [26].

The data analysis is relatively straightforward, as the inclusive scattering at $x > 1$ yields low rates and a small pion background. The trigger and tracking inefficiencies are small and applied as a correction to the measured yield. Electrons are identified by applying cuts on the signals from both the Čerenkov detector and the calorimeters. The cuts yield $> 99\%$ electron efficiency with negligible pion contamination. The overall dead-time of the data acquisition system (DAQ) was evaluated on a run-by-run basis. To ensure a well-understood acceptance, the solid angle and momentum acceptance were limited to high-acceptance regions and a model of the HRSs [26] was used to apply acceptance corrections.

The scattered electron momentum, in-plane and out-of-plane angles, and vertex position at the target can be reconstructed from the VDC tracking information using the optics matrices determined in earlier experiments. For the right HRS, the third quadrupole was unable to run at its full current, and so data were taken in a modified tune with at 15% reduction in its field. Optics data were taken to correct for the modified tune. Many of the systematic uncertainties in the spectrometers are correlated, so we took the conservative approach of applying these uncertainties to the combined result from the HRS-L and HRS-R data.

The cryogenic targets have a large background from scattering in the cell walls. We apply a ± 7 cm cut around the center of the target, removing $> 99.9\%$ of the events from target endcap scattering, as determined from measurements on empty target cells. One of the largest contributions to the systematic uncertainty comes from target density reduction due to heating of the ${}^2\text{H}$, ${}^3\text{He}$, and

${}^4\text{He}$ targets because of the high-current electron beam. We made dedicated measurements over a range of beam currents and used the variation of the yield to measure the current dependence of the target density. The effect was large and varied with the position along the target, and the measurements were used to determine the density loss and thus the effective target thicknesses of the measurement. Since much of the model dependence will be target independent, a conservative 5% normalization uncertainty was applied on the ratio of cryotargets to account for target density uncertainties.

The measured events, corrected for inefficiencies and normalized to the integrated luminosity, were binned in x and compared to the simulated yield. The simulation uses a y -scaling cross section model [16, 27] with radiative corrections applied using the peaking approximation [26, 28]. Coulomb corrections are applied within an improved effective momentum approximation [29], and are 2% or smaller for all data presented here. The combined systematic uncertainty, neglecting the normalization uncertainty due to target thickness uncertainty, is XX-YY%, and is generally the largest contribution to the uncertainties in the ratios except at larger x values where the statistical uncertainty becomes larger.

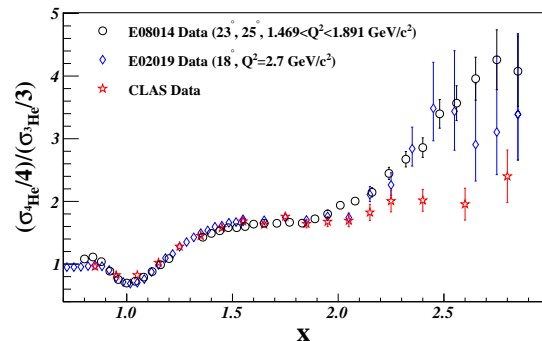


FIG. 1. (Color online) The ${}^4\text{He}/{}^3\text{He}$ cross section ratio for $Q^2 > 1.4 \text{ GeV}^2$ (23° and 25° scattering), along with results from CLAS [14] and Hall C (E02-019) [15]. The error bars include statistical and systematic uncertainties; the global 5% normalization uncertainty is not shown.

Figure 1 presents the ${}^4\text{He}/{}^3\text{He}$ cross section ratio for our $Q^2 > 1.4 \text{ GeV}^2$ data. In the 2N-SRC region, our data are in good agreement with the CLAS [14] and E02-019 [15] results, revealing a plateau for $1.5 < x < 2$. At $x > 2$, our ratios are significantly larger than the CLAS data, but consistent within uncertainties with the E02-019 results. This is consistent with the explanation provided in a recent comment [30] which concluded that the observed plateau was likely the result of large bin-migration effects resulting from the limited CLAS momentum resolution.

While the rise in the ratio above $x = 2$ indicates contributions beyond 2N-SRCs, we do not observe the 3N-SRC plateau expected in the naive SRC model. In this model,

the prediction of scaling as an indication of SRC dominance is a simple and robust way to test for 2N-SRCs, but it is less clear how well it can indicate the presence of 3N-SRCs. For 2N-SRCs, one can predict *a priori* where the plateau should be observed since for a given Q^2 value, x can be chosen to require a minimum nucleon momentum above the Fermi momentum, strongly suppressing single-particle contributions. It is not clear what values of x and Q^2 are required to suppress 2N-SRC contributions well enough to isolate 3N-SRCs; much larger Q^2 values may be required to isolate 3N-SRCs and see analogous plateaus at $x > 2.5$.

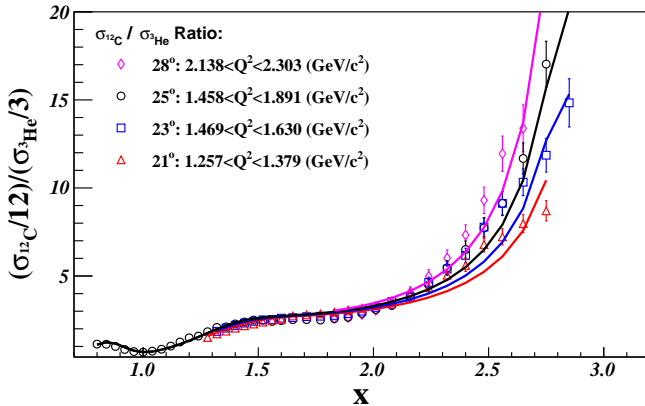
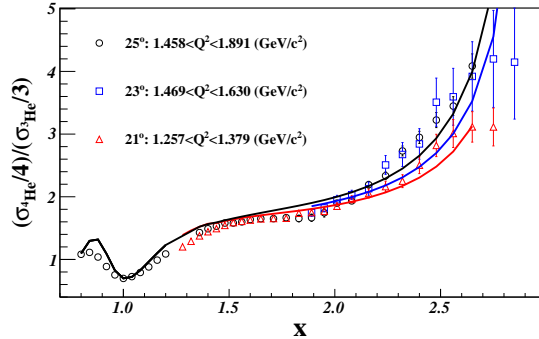


FIG. 2. (Color online) The $^4\text{He}/^3\text{He}$ (top) and $^{12}\text{C}/^3\text{He}$ (bottom) cross section ratios for all angles, along with results from CLAS [14] and Hall C (E02-019) [15] measurements. The solid lines correspond to a simple cross section model based on parameterized momentum distributions.

For 2N-SRCs, the plateau must eventually disappear as the deuteron cross section falls to zero for $x \rightarrow M_D/M_p \approx 2$, causing the $A/2\text{H}$ ratio to rise sharply to infinity. Both the previous high- Q^2 deuterium data and our simple cross section model, based on a parameterization of the nucleon momentum distribution in the nucleus, show that the sharp drop of the deuteron cross section does not occur until $x \approx 1.9$, resulting in a clear plateau for $1.5 < x < 1.9$. For ^3He , our cross section model shows a similar falloff of the ^3He cross section starting near $x \approx 2.5$, thus yielding a rise in the $A/3\text{He}$ ratio that sets in at much lower x values. This rapid rise in the $A/3\text{He}$ ratio as one approaches the ^3He kinematic thresh-

old shifts to lower x as Q^2 increases, as seen in both the data and model in Fig 2. So while the plateau is expected to set in at lower x values as Q^2 increases, as seen in the 2N-SRC region [8, 14], the large- x breakdown also shifts to lower x values. Thus, it is not clear whether higher Q^2 measurements will yield a clean way to isolate and study 3N-SRCs.

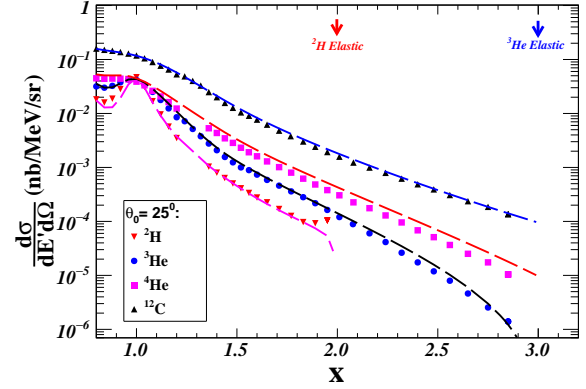


FIG. 3. (Color online) Cross sections of ^2H , ^3He , ^4He and ^{12}C at 25° . The uncertainties include statistical and systematic uncertainties. The normalization uncertainties, ranging from 2-5%, are not shown.

The absolute cross sections for scattering from ^3He , ^4He and ^{12}C at a scattering angle of 25° are shown in Fig. 3. The ^3He cross section falls more rapidly than the other nuclei for $x > 2.5$, yielding the rise in the $^4\text{He}/^3\text{He}$ ratios discussed above. In the naive SRC model, it is assumed that the high- x cross section comes from the contributions of stationary 2N- and 3N-SRCs. The prediction of scaling in this model breaks down due to the difference between stationary SRC in ^2H (or ^3He) and moving SRCs in heavier nuclei. For the most recent extraction of 2N-SRCs from the $A/2\text{H}$ ratios [15], the effect of the 2N-SRC motion in heavier nuclei was estimated and found to give a small enhancement of the ratio in the plateau region, with little distortion of the shape until $x > 1.9$ [15] where the ratio rises rapidly to infinity. For 3N-SRCs, motion of the correlations produces a similar rise which begins well before the kinematic limit at $x \approx 3$. This picture is also consistent with the observation that the $x > 2.5$ increase in the ratio is larger for $^{12}\text{C}/^3\text{He}$. However, a clear interpretation of the large x behavior of $^{12}\text{C}/^3\text{He}$ is more difficult. At very large x values, where the cross section drops rapidly, the data are very sensitive to the spectrometer resolution. When comparing two thin targets, or two extended targets, the acceptance and resolution effects cancel, strongly suppressing such effects in the target ratios. However, in the ratio of $^{12}\text{C}/^3\text{He}$, the variation of the resolution with target length and the possible impact of correlations between the scattering angles and the reconstructed target position can yield different resolution effects for the two targets. So while the rise

in the $^{12}\text{C}/^3\text{He}$ can be explained by the comparison of moving 3N-SRCs to stationary ones, there can be additional effects due to the difference in resolution between the foil targets and the 20cm ^3He targets.

We have performed high-statistics measurements of the $^4\text{He}/^3\text{He}$ and $^{12}\text{C}/^3\text{He}$ cross section ratios, confirming the results of the low-statistics measurements from Hall C [15] and showing a clear disagreement with the CLAS data [14]. This supports the idea that the CLAS data were limited at large x by bin-migration effects due to the spectrometer's modest momentum resolution [30]. We do not observe the plateau predicted by the naive SRC model, but explain why the prediction for the inclusive ratios in the 3N-SRC regime are not as robust as those for 2N-SRC. While we do not observe the predicted plateau, this does not demonstrate that 3N-SRCs are unimportant in this region. Even if the cross section is dominated by 3N-SRCs, the inclusive scattering ratios may not show a plateau due to the motion of the 3N-SRCs.

While the $A/^3\text{He}$ ratios do not provide a direct signature of 3N-SRCs, it should still be possible to use inclusive scattering to look for contributions of 3N configurations in nuclei. The biggest obstacle appears to be the limited region in x where the correction for the motion of any 3N-SRCs in heavy nuclei is small. This problem can be avoided if one compares the ^3He scattering at large x with a model of the contributions of moving 2N-SRCs in ^3He . The contribution of 3N-SRCs would appear as an increase in the cross section relative to what is expected when modeling scattering from ^3He in terms of single-particle strength and 2N-SRC contributions, including precise, quantitative corrections for the motion of the 2N-SRCs. However, because this is a comparison to theory, rather than a comparison of SRCs within two nuclei, one can no longer rely on final-state interactions canceling in the comparison, and these effects would have to be modeled.

It will be important for such comparisons to be performed over a range of Q^2 , making the data to be taken at Jefferson Lab after the energy upgrade important for such studies [31]. In addition, comparisons of scattering from ^3He and ^3H at large x [32] allow for comparison of the isospin structure in the high-momentum components of the ^3H and ^3He nucleon momentum distributions. If only 2N-SRCs contribute at large momenta, then the observed n-p pair dominance will yield nearly identical cross sections for the $x > 2$ region as well, while contributions from 3N-SRCs need not be isospin independent.

We would like to acknowledge the outstanding support from the Jefferson Lab Hall A technical staff and the JLab target group. This work was supported in part by the DOE Office of Science, Office of Nuclear Physics, contract DE-FG02-96ER40950, under which JSA, LLC operates JLab, DOE contracts DE-AC02-06CH11357,

DE-AC05-06OR23177, the National Science Foundation, and the UK Science and Technology Facilities Council (ST/J000175/1, ST/G008604/1).

* deceased

- [1] T. DeForest, Nucl. Phys. **A392**, 232 (1983).
- [2] G. Van Der Steenhoven *et al.*, Nucl. Phys. **A480**, 547 (1988).
- [3] L. Lapikas, Nucl. Phys. A **553**, 297 (1993).
- [4] J. Kelly, Adv. Nucl. Phys. **23**, 75 (1996).
- [5] J. Carlson *et al.*, (2014), 1412.3081.
- [6] Z. T. Lu *et al.*, Rev. Mod. Phys. **85**, 1383 (2013).
- [7] L. Frankfurt and M. Strikman, Physics Reports **76**, 215 (1981).
- [8] L. L. Frankfurt, M. I. Strikman, D. B. Day, and M. Sargsyan, Phys. Rev. C **48**, 2451 (1993).
- [9] J. Arrington, D. Higinbotham, G. Rosner, and M. Sargsian, Prog. Part. Nucl. Phys. **67**, 898 (2012).
- [10] O. Benhar, D. Day, and I. Sick, Rev. Mod. Phys. **80**, 189 (2008).
- [11] C. Ciofi degli Atti and S. Simula, Phys. Rev. C **53**, 1689 (1996).
- [12] R. Wiringa, R. Schiavilla, S. C. Pieper, and J. Carlson, Phys. Rev. **C89**, 024305 (2014).
- [13] K. S. Egiyan *et al.*, Phys. Rev. **C68**, 014313 (2003).
- [14] K. S. Egiyan *et al.*, Phys. Rev. Lett. **96**, 082501 (2006).
- [15] N. Fomin *et al.*, Phys. Rev. Lett. **108**, 092502 (2012).
- [16] J. Arrington *et al.*, Phys. Rev. Lett. **82**, 2056 (1999).
- [17] J. Arrington *et al.*, Phys. Rev. **C64**, 014602 (2001).
- [18] J. L. Aclander *et al.*, Phys. Lett. **B453**, 211 (1999).
- [19] A. Tang *et al.*, Phys. Rev. Lett. **90**, 042301 (2003).
- [20] R. Subedi *et al.*, Science **320**, 1476 (2008).
- [21] I. Korover *et al.*, Phys. Rev. Lett. **113**, 022501 (2014).
- [22] O. Hen *et al.*, Science **346**, 614 (2014).
- [23] E. Piasetzky, M. Sargsian, L. Frankfurt, M. Strikman, and J. W. Watson, Phys. Rev. Lett. **97**, 162504 (2006).
- [24] J. Arrington, D. Day, D. Higinbotham, and P. Solvignon, Three-nucleon short range correlations studies in inclusive scattering for $0.8 < Q^2 < 2.8(\text{GeV}/c)^2$, <http://hallaweb.jlab.org/experiment/E08-014/>, 2011.
- [25] J. Alcorn *et al.*, Nucl. Instrum. Meth. **A522**, 294 (2004).
- [26] Z. Ye, Ph.D Thesis, University of Virginia, 2013, arXiv:1408.5861.
- [27] D. B. Day, J. S. McCarthy, T. W. Donnelly, and I. Sick, Annual Review of Nuclear and Particle Science **40**, 357 (1990).
- [28] S. Stein *et al.*, Phys. Rev. **D12**, 1884 (1975).
- [29] A. Aste, C. von Arx, and D. Trautmann, Eur. Phys. J. **A26**, 167 (2005).
- [30] D. W. Higinbotham and O. Hen, Phys. Rev. Lett. **114**, 169201 (2015).
- [31] J. Arrington, D. Day, N. Fomin, and P. Solvignon, Inclusive scattering from nuclei at $x > 1$ in the quasielastic and deeply inelastic regimes, Jefferson Lab Experiment Proposal E12-06-105, 2006.
- [32] J. Arrington, D. Day, D. W. Higinbotham, and P. Solvignon, Precision measurement of the isospin dependence in the 2N and 3N short range correlation region, Jefferson Lab Experiment Proposal E12-11-112, 2011.